SOME PROPERTIES OF THE Ba_2SiO_4 OXIDE CATHODE INTERFACE

A. EISENSTEIN

TECHNICAL REPORT NO. 80

AUGUST 19, 1948

RESEARCH LABORATORY OF ELECTRONICS

MASSACHUSETTS INSTITUTE OF TECHNOLOGY

The research reported in this document was made possible through support extended the Massachusetts Institute of Technology, Research Laboratory of Electronics, jointly by the Army Signal Corps, the Navy Department (Office of Naval Research) and the Air Force (Air Materiel Command), under Signal Corps Contract No. W-36-039-sc-32037, Project No. 102B; Department of the Army Project No. 3-99-10-022.

MASSACHUSETTS INSTITUTE OF TECHNOLOGY

Research Laboratory of Electronics

Technical Report No. 80 August 19, 1948

SOME PROPERTIES OF THE Ba_2SiO_4 OXIDE CATHODE INTERFACE

A. Eisenstein

Abstract

Oxide cathodes prepared on a Si-Ni alloy base metal have at the interface barium orthosilicate. The thickness of this layer is measured by means of an x-ray method and found to increase with the life of the cathode and to be of the order of 10^{-3} cm. Measurements of the effective, specific electrical conductivity were made and compared with the conductivity of the coating, (BaSr)O. Both materials exhibit a conductivity-temperature variation characteristic of semi-conductors; however, the conductivity of the interface was always less than that of the coating. The interface layer influences the thermionic emission characteristics of the cathode because of an interface voltage developed by the flow of emission current. A retarding-potential method is developed for determining this voltage.

SOME PROPERTIES OF THE Ba_2SiO_4 OXIDE CATHODE INTERFACE

Introduction

The oxide cathode interface lying between the base metal and the oxide coating is now regarded as an important cathode parameter although the specific influence of the interface on thermionic emission is not completely clear. Undoubtedly the type of interface and the conditions under which emission is taken allow the role of the interface to change. The interface region may arise from one of several physical conditions; yet all types are expected to have somewhat similar electronic properties. If the oxide coating is considered to be an impurity semiconductor, the absence of activation centers in the coating immediately adjacent to the base metal may act as a blocking layer[1] to the normal flow of electrons. Poor mechanical bonding[2] of the coating to the base metal gives rise to a thin vacuum layer between the two and may also behave as a blocking layer. Solid-state chemical reactions between the oxide coating and constituents of the base metal frequently give rise to interface compounds whose electrical properties differ from those of the coating. If the conductivity of this interface material is very low, it may act as a blocking layer. These interface forms behave as a series element to the normal flow of electrons from the base metal to the coating; accordingly, a voltage drop[3] should appear across the interface region when a thermionic emission current is taken from the cathode. In this discussion we shall be concerned with the properties of only those interface layers which differ in chemical constitution from the oxide coating and are thus easily detected.

Chemical, spectroscopic, and x-ray diffraction analyses have been used to identify interface compounds, the latter technique giving the most useful information. Rooksby reports[4,5] finding barium aluminate $BaAl_2O_4$ at the interface of cathodes prepared on a 2 per cent Al-Ni alloy base metal. Later studies led to the report[6] of barium orthosilicate Ba_2TiO_4 on a 0.23 per cent Ti-Ni alloy base. MgO was identified[7] in the interface region of cathodes prepared on a Mg-Ni alloy base. Fineman and Eisenstein[8] studied interfaces formed on Cr-Ni alloys and chromium-plated nickel. Three possible interface compounds were reported, only one of which was stable in air. Although this compound exhibited a closely packed hexagonal structure, none of these interface compounds was chemically identified. X-ray diffraction patterns from the interface region of cathodes prepared on a pure nickel base material show only very weak diffraction lines; hence it seems unlikely that interface compounds are present in this type of cathode.

From this group of interface compounds, barium orthosilicate was selected for a detailed study, since (1) it was chemically stable and easy to synthesize, and (2) it was known to influence the thermionic emission properties of the cathode. A complete study of the influence of the interface layer on the electronic properties of the cathode must include information on the effective electrical conductivity of the interface compound and values of the effective thickness of the interface layer as well as thermionic emission data.

1. Interface Formation

The Ba_2SiO_4 interface present in cathodes prepared on a Si-Ni alloy base arises from a chemical reaction between silicon in the base metal and BaO in the coating. Although most oxide coatings contain both barium and strontium, e.g. (BaSr)O, only barium enters into the interface compound.[6,8] When a pure SrO coating is used, a strontium orthosilicate Sr_2SiO_4 interface is formed. The presence of either of these compounds is easily verified by removing the oxide coating[8] and taking x-ray diffraction patterns of the underlying material. O'Daniel and Tscheischwili report[9] the structure of the orthosilicates as being similar to that of K_2SO_4 with the space group D_{2h}^{16}. Ba_2SiO_4 has lattice constants a = 5.7, b = 10.1, and c = 7.5 angstroms. Solid solutions of $(BaSr)_2SiO_4$ are known to occur, although these are not found at the oxide cathode interface.

When the coating is removed from the cathode, the presence of the Ba_2SiO_4 interface is readily apparent by its grey color. The fact that interfaces are easily observed and give good x-ray diffraction patterns, as well as details of its electrical behavior, led Wright[7] to predict a probable interface thickness range of 10^{-4} to 10^{-5} cm. More recent but unpublished results[10] obtained by Rooksby place this interface thickness at 10^{-3}cm.

An x-ray technique for measuring the thickness of thin crystalline films has been described.[11] This method is based on a comparison of the integrated intensities of x-ray diffraction lines scattered from a thin crystalline surface film and from an underlying crystalline base material. A direct application of this technique to a measurement of the interface thickness is possible only when the absorption coefficient and the crystal structure of the interface material are known. A comparison technique was adopted for evaluating the thickness of the Ba_2SiO_4 interfaces.

Synthetic Ba_2SiO_4 was prepared[12] in a solid-state chemical reaction between $BaCO_3$ and SiO_2 (dehydrated silicic acid) at about 1300°K. This powder in a suitable organic binder was sprayed on the surface of a 3mm-diameter nickel sleeve. The effective thickness of the Ba_2SiO_4 layer

was calculated from the weight of the film, the coated area, and the crystalline density[13]: 5.7 gm/cm^3. The true thickness of the film was undoubtedly greater than the calculated effective thickness because of the somewhat lower density of the sprayed coating. No error will occur, however, in the subsequent determination of the actual interface thickness if its density is that of the crystalline solid. X-ray diffraction patterns were taken of the synthetic interface samples with the technique previously described.[8] The sample was rotated continuously during the x-ray exposure to minimize the preferred orientation diffraction spots arising from the large crystal size of the underlying nickel. This technique is essential if accurate measurements of the diffraction line intensity are to be made. Figure 1a shows a set of x-ray diffraction patterns obtained from synthetic

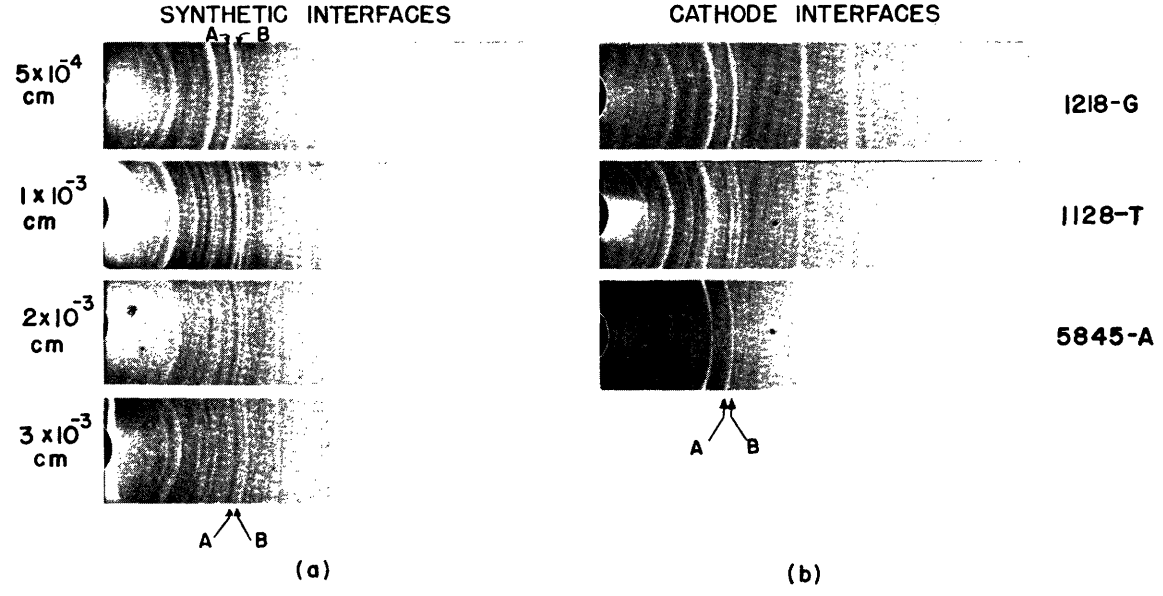

Fig. 1. (a) X-ray diffraction patterns of Ba_2SiO_4 synthetic interface film overlying nickel base metal. Interface thickness 5 x 10^{-4}cm, 10^{-3}cm, 2 x 10^{-3}cm, and 3 x 10^{-3}cm, respectively, reading top to bottom. (b) Diffraction patterns of actual Ba_2SiO_4 cathode interfaces.

interface samples of effective thickness 5 x 10^{-4} cm, 1 x 10^{-3} cm, 2 x 10^{-3} cm, and 3 x 10^{-3}cm. Subsequent thickness measurements were based on a comparison of the integrated intensities of the diffraction lines marked A and B, of the underlying nickel and of the Ba_2SiO_4 surface film, respectively. These lines occur at nearly the same scattering angle and their respective integrated intensities are easily measured by microphotometering this section of the film. Figure 2 shows a log-log plot of the ratio of the integrated intensities of lines A and B as a function of the effective interface thickness. An experimental measurement of the ratio of the integrated intensities of these diffraction lines from actual cathode samples, see Fig. 1b, may be referred to Fig. 2 for an immediate determination of

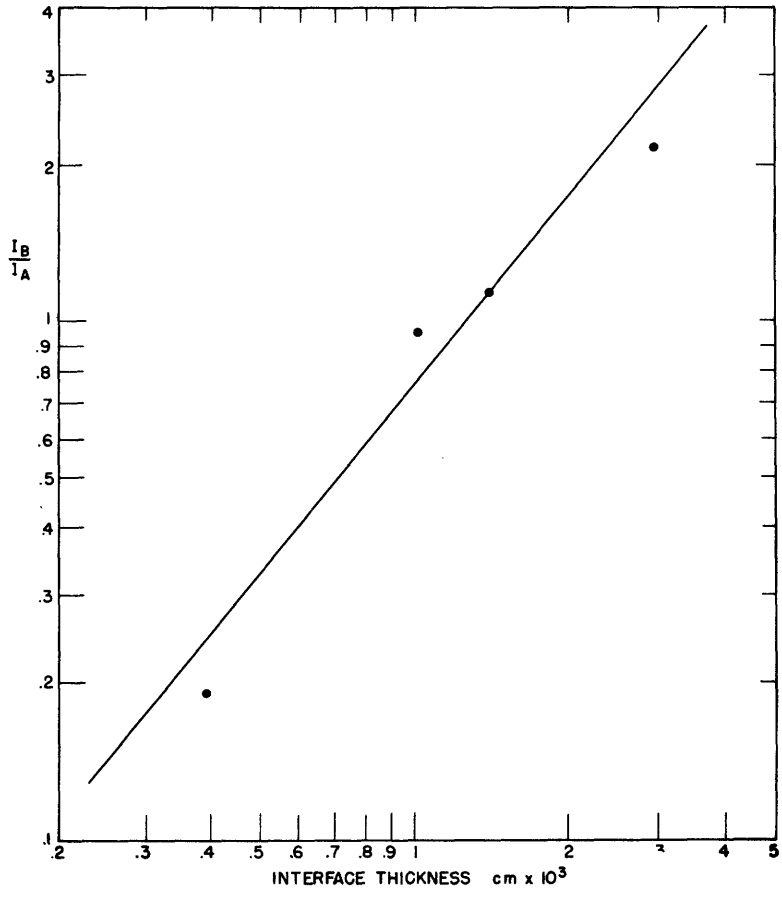

Fig. 2. Ratio of integrated intensities of lines A and B as a function of interface thickness.

the effective interface thickness. A straight line has been drawn through the experimental points as best representing the true behavior since previous work[11] indicated that this log-log function should be linear or have an upward curvature.

If the interface results from a solid-state chemical reaction between constituents of the base metal and the coating, the interface thickness should be a function of the parameters governing the migration of these components. Only one of these, time, has been investigated. Four cathodes were prepared on a 5 per cent Si-Ni alloy base metal which had been chemically cleaned and vacuum-fired. Each was coated with $(BaSr)CO_3$+, to a weight of 10 mg/cm^2, and each processed in a similar manner with a maximum temperature of 1175°K. One tube was set aside as representing the interface thickness immediately following processing and was called zero hours. Two of the tubes were heated at 1125°K without drawing anode current for 50 hours and the remaining tube for 100 hours. Because of the slight solubility of

+ Raytheon C51-2 coating mix.

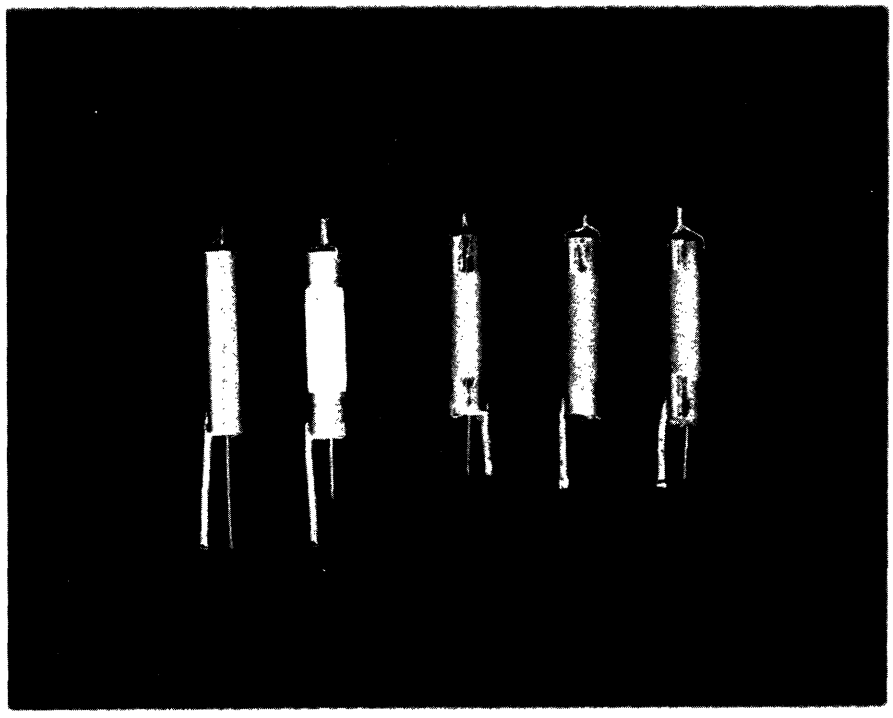

Fig. 3. Reading left to right: uncoated Si-Ni alloy sleeve, normal carbonate coated cathode, barium orthosilicate interface at zero hours, 50 hours, 100 hours.

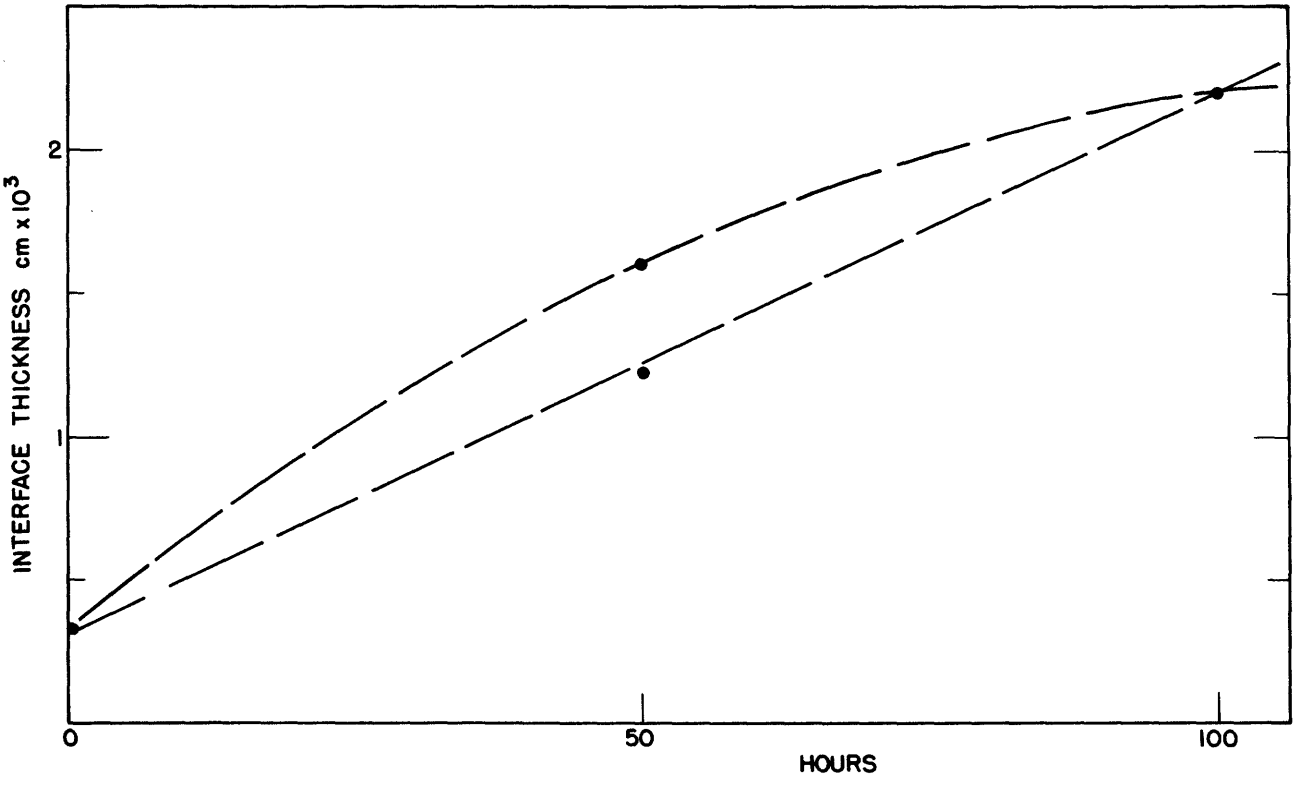

Fig. 4. Variation of interface thickness with time of heating cathode at 1125°K.

Ba_2SiO_4 in water, the coatings were removed by dipping in acetone. The underlying interfaces are shown in Fig. 3. For comparison, a normal coated cathode is also shown. A measurement of the interface thickness of each cathode was made using the method described. These thickness values are plotted as a function of the heating time in Fig. 4. The two tubes at 50 hours indicate the amount of variation to be expected. Unfortunately, this uncertainty does not allow the exact functional relationship to be determined but it seems definite that the interface thickness increases with time and that the order of magnitude of this thickness is 10^{-3} cm. Further studies of this type are being undertaken, for until the factors governing the interface thickness are understood, deductions regarding time effects of the interface on the thermionic emission process are useless.

2. Thermionic Emission Properties

The effect of adding reducing impurities to the base metal of an oxide cathode has been examined and discussed by several investigators.[14,15,16] It is generally believed that the reducing impurities react chemically with the (BaSr)O coating releasing "free" barium which serves as impurity centers in the oxide semi-conductor and perhaps also reduces the dipole moment at the vacuum surface of the oxide. This chemical reaction is also consistent with the F center model of semi-conductor activation which is somewhat more satisfying in some respects[17] than is N-type activation by excess barium. On the basis of the early experiments[14,15,16], one is led to believe that the presence of reducing impurities enhances emission, or the presence of oxidizing impurities or vapors reduces the emission as compared to that obtainable from a pure, uncontaminated nickel base metal. It is now becoming evident that many experiments designed to measure the true d-c emission capabilities of a cathode succeed only in evaluating the state of cathode activity determined in a balance between cathode activation by the reducing impurities and cathode deactivation by vapors from the anode or other tube parts. Jacobs,[18] and Hamaker, Gruining, and Aten[19] have clearly indicated the possibility of anode poisoning in such tubes and Dillinger[2] has demonstrated that extremely high, d-c space-charge-limited emission-current densities may be taken from a pure nickel base cathode, one value being 19 amp/cm^2 at about 1150°K. The probability of anode poisoning is somewhat reduced in measurements of pulsed emission. Coomes[20] reports the one-microsecond pulsed emission-current densities which may be obtained from cathodes prepared on a pure nickel base to exceed the emission-current densities from cathodes on the electronic grade A nickel[15] containing various reducing impurities. This study represents a comparison of the sparking current densities and does not necessarily serve as a measure of the cathode's intrinsic activity.

A comparison of the microsecond pulsed voltage-current characteristics of cathodes prepared on a pure nickel and on either a 2 per cent or

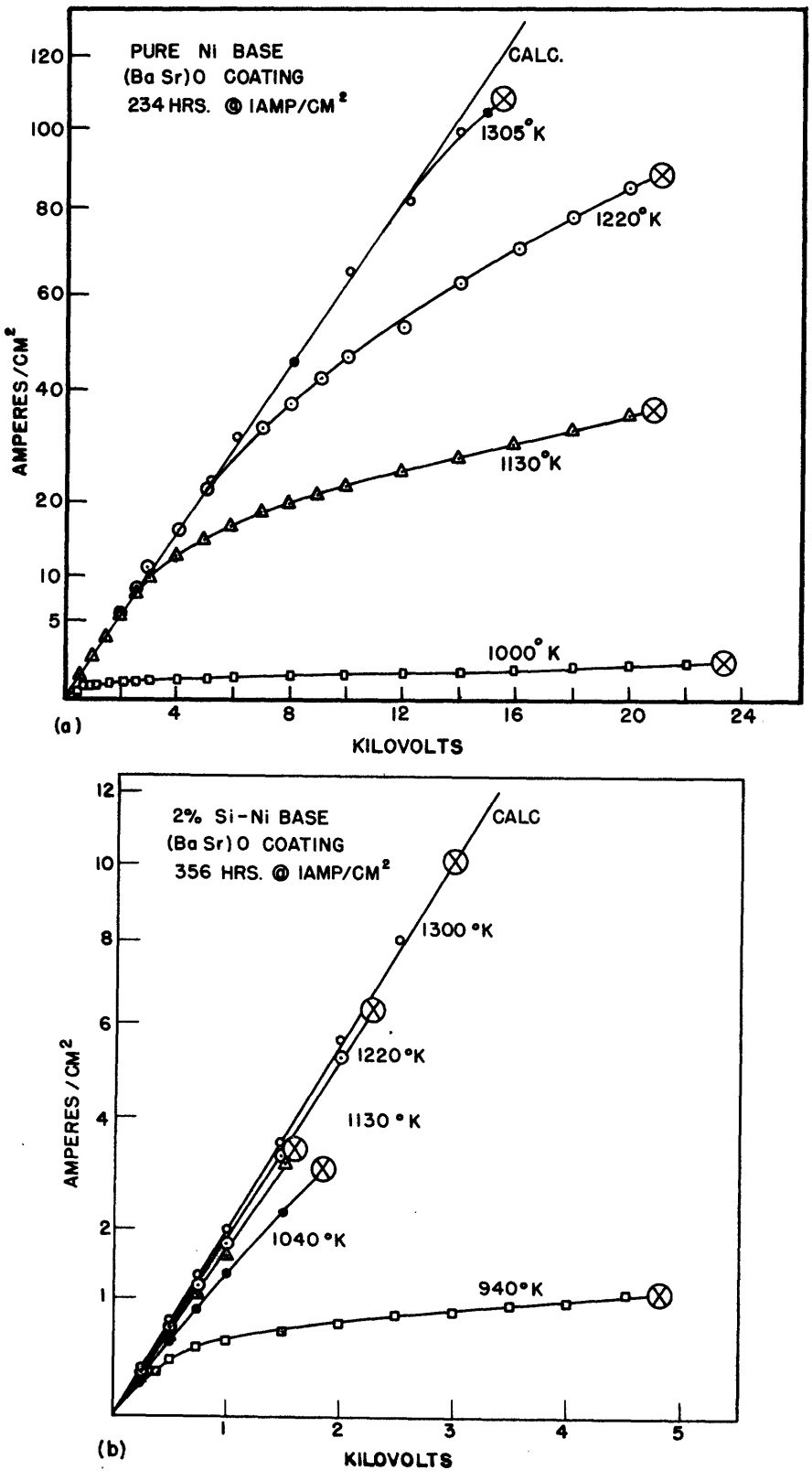

Fig. 5. Voltage-current pulsed-emission characteristics of cathodes prepared on (a) pure nickel base, and (b) 5 per cent alloy base. Current plotted on a 2/3 power scale.

a 5 per cent Si-Ni alloy base and tested in the laboratory diode[21] shows two obvious differences, (see Fig. 5). For a given temperature the sparking current density, representing the maximum practical limit of emission, is seen to be considerably higher for the pure nickel base cathode than for the alloy base cathode. At 1300°K the 110 amp/cm^2 sparking current densities were 110 amp/cm^2 and 10 amp/cm^2, respectively, for the two types. As the temperature is reduced, the point of departure from the calculated Langmuir-Child space-charge-limited emission line is seen to decrease, following a Richardson type of behavior for the pure nickel base cathode. The alloy base cathode shows no sharp departure from the space-charge line but rather a change in slope, the apparent point of departure occurring at near zero current density. This "progressive deviation" from the space-charge line at reduced temperatures and the low values of the sparking current density are believed to be characteristic of the interface type cathode and to be directly associated with a sizeable interface voltage drop which occurs when high pulsed currents are passed through the interface layer.

Further confirmation was sought to show that the two characteristics, the progressive deviation and the low sparking current density, are due to the interface layer rather than to a different state of coating activity brought about by the presence of Si in the base metal. A cathode was prepared in which a layer of synthetic Ba_2SiO_4 was applied to a pure nickel base and over this was sprayed a normal coating of $(BaSr)CO_3$. The effective Ba_2SiO_4 interface thickness was 6×10^{-4} cm and the coating weight was 10 mg/cm^2. The interface layer extended considerably beyond the oxide-coated width to prevent possible direct contact between the oxide coating and base metal, (see Fig. 6). Figures 7a,b show microsecond pulsed voltage-current emission characteristics of this cathode at two stages of cathode life. The cathode was held at 1150°K and a d-c emission current density of 1 amp/cm^2 was drawn during the life-test period. Both of the emission

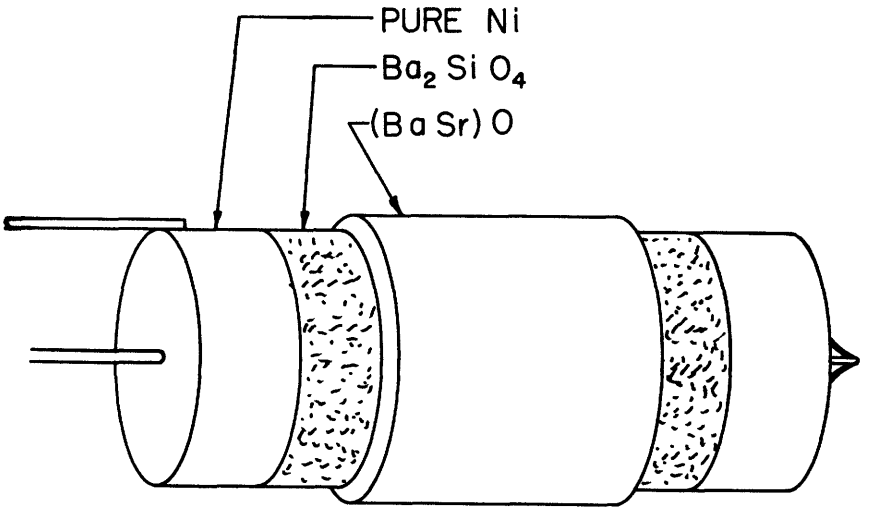

Fig. 6. Sketch showing construction of synthetic interface cathode, (see text).

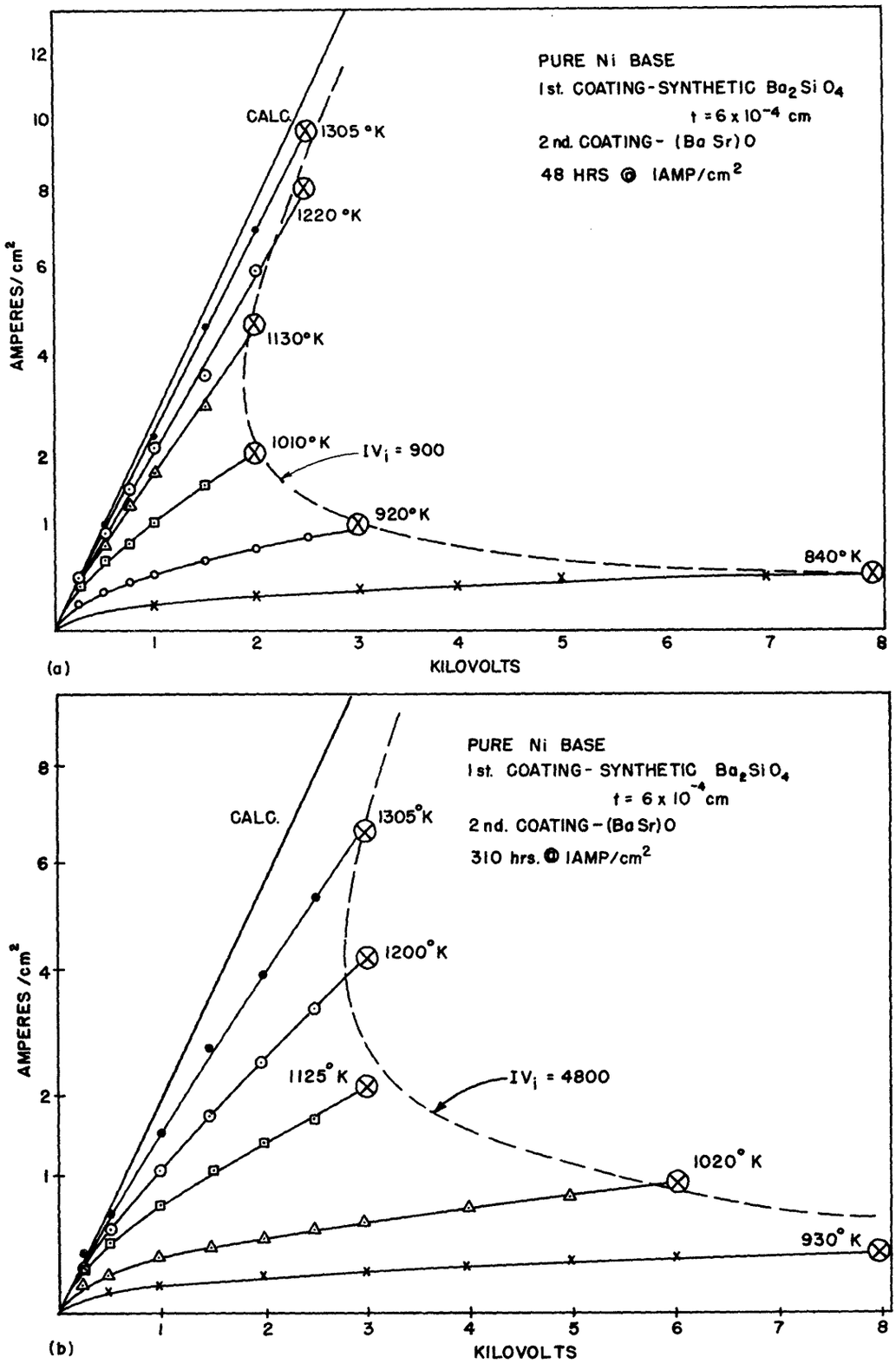

Fig. 7. Voltage-current, pulsed-emission characteristics of synthetic interface cathode (a) at 48 hours, (b) at 310 hours.

characteristics are seen to show the progressive deviation and the low spark-current densities previously found in normal Ba_2SiO_4 interface cathodes. Thus it was concluded that these characteristics result from the presence of the silicate interface layer.

A comparison was made of the emission capabilities of the pure nickel base cathode and the Si-Ni alloy base cathode over an extended period of cathode life. Ten laboratory diodes were used in this comparison; five of the cathodes were prepared on pure nickel, three on a 5 per cent Si-Ni alloy base and two on a 2 per cent Si-Ni alloy base.+ All of the cathodes were coated with $(BaSr)CO_3$ to a weight of about 10 mg/cm^2 and processed in a similar manner, with a maximum temperature of 1225°K. Microsecond pulse emission characteristics were recorded at periodic intervals during the life test. Cathodes were operated at a corrected temperature of 1150°K during both the pulse emission measurement and the life-test period. A d-c emission current density of 1 amp/cm^2 was drawn from the cathodes during the life test. Figure 8 shows the variation of the sparking current density with the life of the cathode. Wide variations are seen among the tubes,

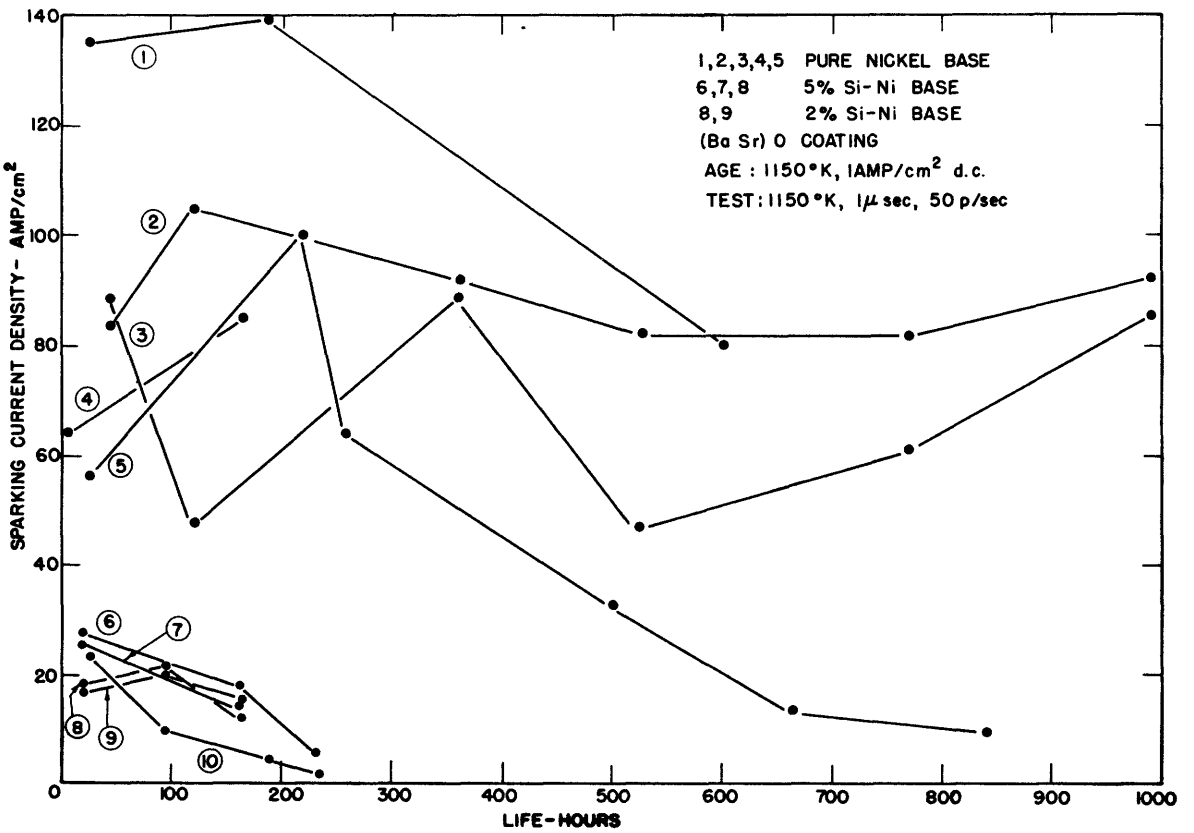

Fig. 8. Variation of sparking-current density with life for pure nickel base cathodes and Si-Ni base cathodes.

+ All of the cathode base materials were kindly supplied by E. M. Wise of the International Nickel Co. The pure nickel was prepared electrolytically and contained no added impurities.

and fluctuations occur in the emission of a single cathode with life. Nevertheless, the sparking current densities of the alloy base cathodes are considerably less than are those of the pure nickel base cathodes. Furthermore, the emission values for the two types of alloy base are nearly the same and show a more rapid decline with increasing cathode life than is found for the pure nickel base. This rapid reduction in the sparking current density may well be due to a change in the interface conductivity or thickness.

No evidence was found for a decay of emission during the pulse although many of the cathodes were tested with both one and ten microsecond pulses. This result is contrary to the results reported by Sproull[22] who found a marked emission decay in the microsecond range for cathodes at 1100°K.

3. Conductivity

If the oxide cathode interface gives rise to the progressive deviation type of emission characteristic and controls the sparking current density through the development of a high interface voltage, one would expect the electrical conductivity of the interface material to be somewhat less than that of the coating. Numerous experiments[23] have been conducted to evaluate the electrical conductivity of the oxide coating and its temperature variation. Many of these pertain to an unknown state of cathode activity or to bulk samples of the oxides; hence, measurements of the oxide coating conductivity as well as the conductivity of Ba_2SiO_4 seemed desirable.

Measurements of the conductivity of these materials were made in tubes of the type shown in Fig. 9. $(BaSr)CO_3$ or synthetically prepared Ba_2SiO_4 in a suitable organic binder were sprayed on the surface of a MgO ceramic rod.+ Half of the desired coating weight was applied and four platinum strips 0.001 in. thick and 2 mm wide were clamped around the sprayed ceramic with the center strips separated by about 15 mm. The remainder of the coating was applied, the platinum bands being left imbedded in the coating. An internal tungsten heater was passed through two axial holes in the ceramic rod. This assembly in cross section is shown in the upper right of Fig. 9. The sample was mounted at the center of a tantalum can which completely surrounded the rod except for two small viewing holes in the side and a slit in the top through which passed the electrical leads. A radio-frequency induction coil surrounded the tube and was used to heat the can which acted as a uniform temperature "furnace" for the sample. The temperature of the can could be made uniform to within 5°C by suitably spacing the turns of the coil. As a check on the temperature, a 0.002-in. tungsten wire was welded to

+ The high purity MgO rods were supplied by A. H. White of the Bell Telephone Laboratories and are a type which were developed for their conductivity studies of oxide coatings. The rod was thoroughly outgassed in vacuum at 1300°K before the coating was applied.

probe lead number 2. The temperature recorded with this thermocouple was found to be in disagreement by a maximum of 20°C with the assumed black-body radiation temperature as observed through the side holes with an optical pyrometer. A water bath surrounding the thermocouple press of the tube served as the cold thermocouple junction, (see Fig. 9). For heat treatment in gases, the sample was heated by means of the internal tungsten heater, leads 1 and 4. Conductivity measurements were made by passing a current between probes 5 and 7 and measuring the potential developed between probes 2 and 3 with a potentiometer circuit. The effective specific conductivity of the material between probes 2 and 3 could be evaluated from the equation

$$\sigma = \frac{i\ell}{Vct} \qquad (1)$$

where i is the current passing between probes 5 and 7, ℓ is the distance between probes 2 and 3, V is the potential developed between probes 2 and 3, c is the circumference of the coated ceramic and t is the coating thickness. Conductivities determined in this manner showed no dependence on the current density except at values approaching 1 amp/cm^2 which resulted in a heating of the coating. Measurements were generally made with a current density of 10 ma/cm^2 with the tube continuously exhausted at a pressure of less than 10^{-7} mm. Typical results obtained in the study of equal molar (BaSr)O are shown in Fig. 10. The effective specific conductivity in reciprocal ohm-cm is plotted logarithmically as a function of the reciprocal temperature in degrees Kelvin. Sample C-13 was activated at a temperature of 1225°K by passing current densities up to 1 amp/cm^2, and the conductivity measurements were taken on three successive days. These curves in sequence comprise Fig. 10a. Over a considerable temperature range the experimental values may be represented by a straight line. This indicates an exponential variation of the type

$$\sigma = Ke^{-Q/kT} \qquad (2)$$

The similarity between this and the theoretical expression[24] for the temperature dependence of conductivity for semi-conductors is easily recognized:

$$\sigma = \frac{4\sqrt{2}}{3} n_b^{\frac{1}{2}} \frac{e^2 \ell_o}{h^{3/2}} (2\pi m^* kT)^{1/4} e^{-\Delta\epsilon/2kT} \qquad (3)$$

where n_b = density of impurity centers

ℓ_o = mean free path

$\Delta\epsilon$ = energy gap separating the bottom of the conduction band and the impurity levels

e, h, m*, k, and T have their usual significance.

The energy Q, obtainable from the slopes of the curves of Fig. 10 is related to the thermal activation energy $\Delta\epsilon$ by

$$Q = \tfrac{1}{2}\,\Delta\epsilon. \qquad (4)$$

Values of $\Delta\epsilon$ of 0.52, 0.71, and 0.71 electron volts were thus obtained respectively from the three curves of Fig. 10a.[+]

Activation of sample C-14 by the passage of a high current density is seen in Fig. 10b. An upward shift of the curves accompanied by a decrease of slope attends this activation. In the initial, unactivated state the thermal activation energy is 3.22 ev and decreases to 0.95 ev after the passage of a 0.5 amp/cm^2 current density for 30 minutes and 1 amp/cm^2 for one hour. Some time later this sample showed an activation energy of 1.17 ev Curve 1, Fig. 10c. The sample was exposed to a few millimeters pressure[++] of CO_2 and heated by means of the internal tungsten coil to 1100°K for a period of 5 minutes. Following this treatment, the tube was quickly exhausted and Curve 2 was taken. Similar treatments for like time and pressure conditions in H_2 and CH_4 resulted in Curves 3 and 4, respectively. Activation and deactivation in the emission from oxide cathodes in CH_4 and CO_2 were discussed by Prescott and Morrison[25] in terms of a chemical reduction of BaO or an oxidation of free barium in the coating. Beneficial effects of H_2 on the activity of cathodes is described[23] by several workers. As in the case of high d-c current activation, the slope of the curve decreased with increasing activity yielding activation energies between 3.37ev and 0.53ev for CO_2 and CH_4 treatments, respectively.

+ Conyers Herring has recently shown that if a semi-conductor model is chosen in which the number of impurity centers exceeds the number of available electrons, the factor of $\frac{1}{2}$ in Eq. (4) should, for a (BaSr)O coating, be replaced by a value near unity.

++ CO_2, H_2 and CH_4 gases used in this experiment were Airco products procured in glass flasks.

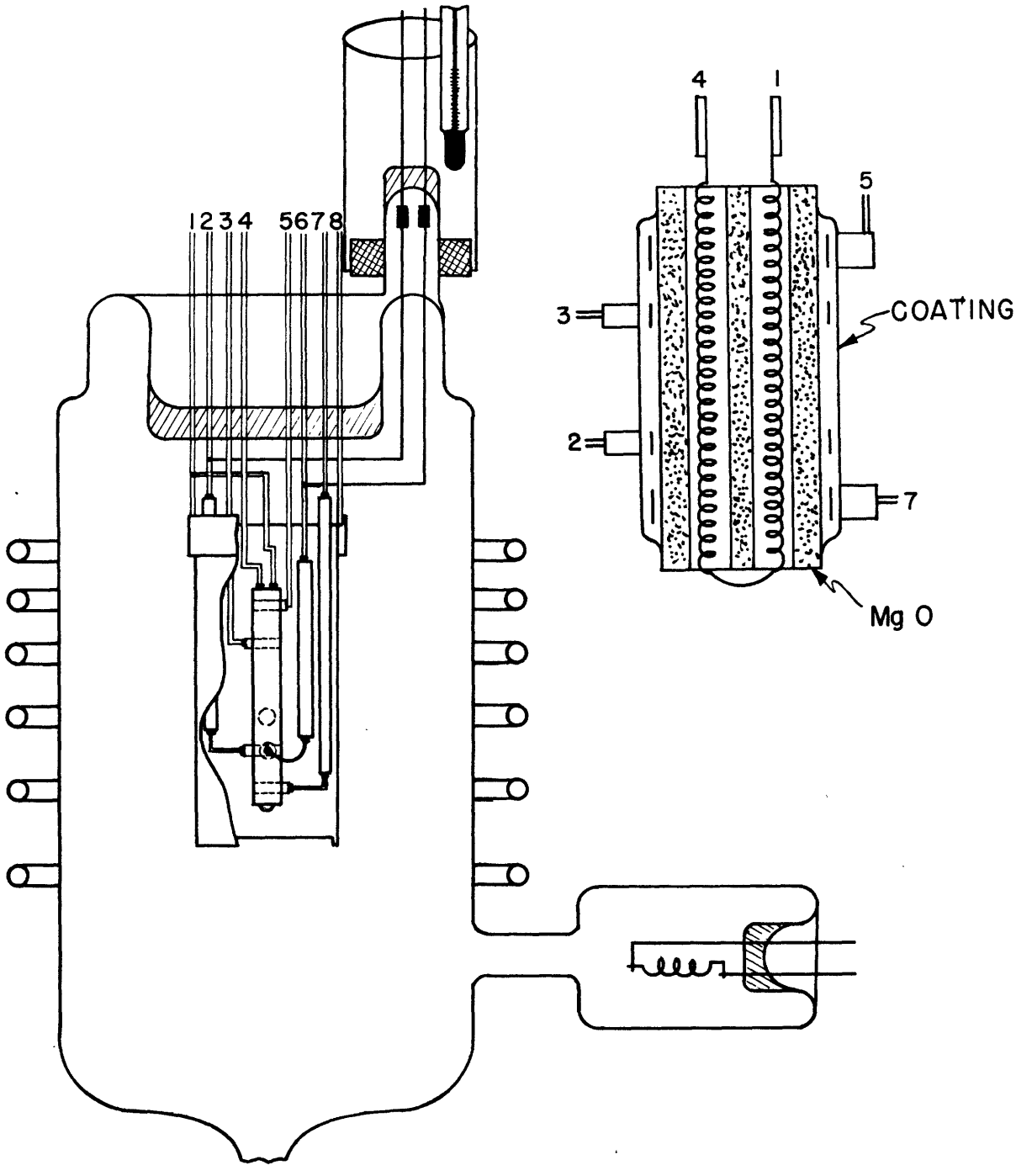

Fig. 9. Tube for measuring electrical conductivity. Enlarged view of the MgO rod is shown at the upper right.

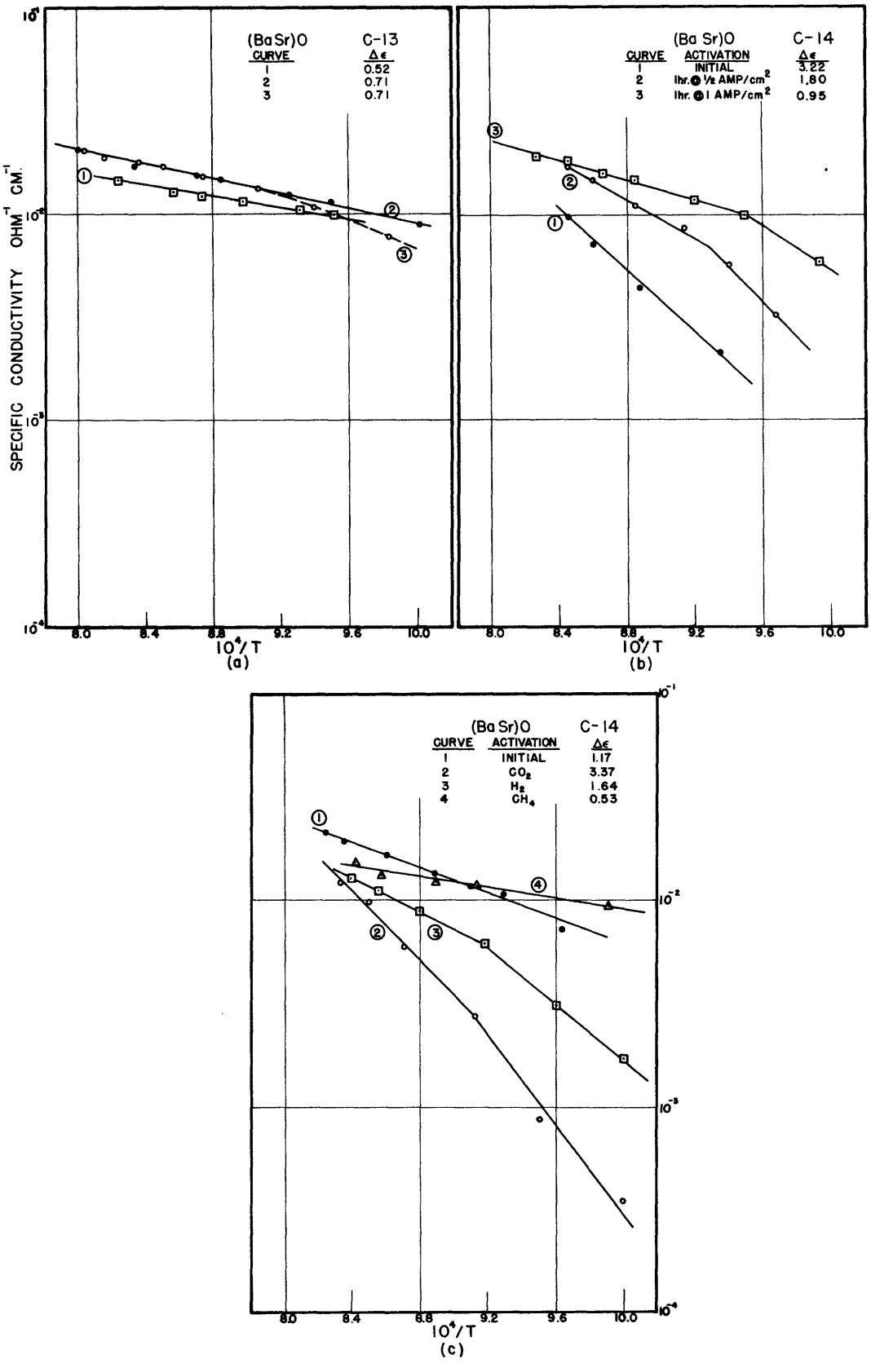

Fig. 10(a), (b), (c). Temperature variation of the electrical conductivity of (BaSr)O, (see text).

A consideration of Eq. (3) indicates that although a change in the free barium content of the sample, n_b, would shift the conductivity curve in the appropriate direction, this change alone should not alter the slope of the curve. Likewise, Eq. (3) offers no explanation for the slight change of slope with temperature observed experimentally in several of the curves. The apparent shift of activation energy with the state of activity and with the temperature is frequently observed in semi-conductors and probably results from the overly simplified model of the semiconductor used in the derivation of Eq. (3). Nijboer[26] and Herring[27] have offered theoretical explanations for the change of slope over different temperature ranges; these are based on a model in which the number of impurity centers exceeds the number of free electrons. Only qualitative explanations are available to explain the decreasing slope of the curve with increasing impurity concentration, n_b. Mott[26] suggests that as the concentration increases a mutual interaction of the electrons bound at impurity centers may result, thus causing a reduction in the binding energy and the value of $\Delta\epsilon$. Any model in which electron traps are located below the impurity levels and are gradually filled as the number of impurity atoms increases, is also capable of justifying the change of slope with concentration.+

The specific conductivity of synthetically prepared Ba_2SiO_4 was measured over the same temperature range by using similar techniques, although a lower conduction current density was used because of the very low conductivity of the material. Immediately following the sample outgassing in vacuum, CO_2 was admitted and a heat treatment carried out to remove the carbon residue from the organic binder. Curve 4, Fig. 11, was taken with the sample again in vacuum and heated by the furnace. A continued heat treatment in vacuum for several hours at 1175°K produced some activation, Curve 5. Passing a high d-c current through the sample resulted in an additional activation, Curve 6. This current was just sufficient to cause a noticeable increase in the temperature of the sample. A slight decrease in conductivity followed a second heat treatment in CO_2, Curve 7. In general, the conductivity behavior of the silicate resembles that of the oxide except that the conductivity values are much lower, and the activation energy is much higher, between 5.2 ev and 7.9 ev. For comparison, the conductivity results from Fig. 10a are shown on the same plot. It is interesting to note that at a temperature of 1250°K the conductivity of the oxide exceeds that of the silicate by a factor of only 10, while at 1000°K this factor is nearly 10,000. Any interface phenomena depending upon a voltage

---

+ Suggested by J. A. Burton, Bell Telephone Laboratories.

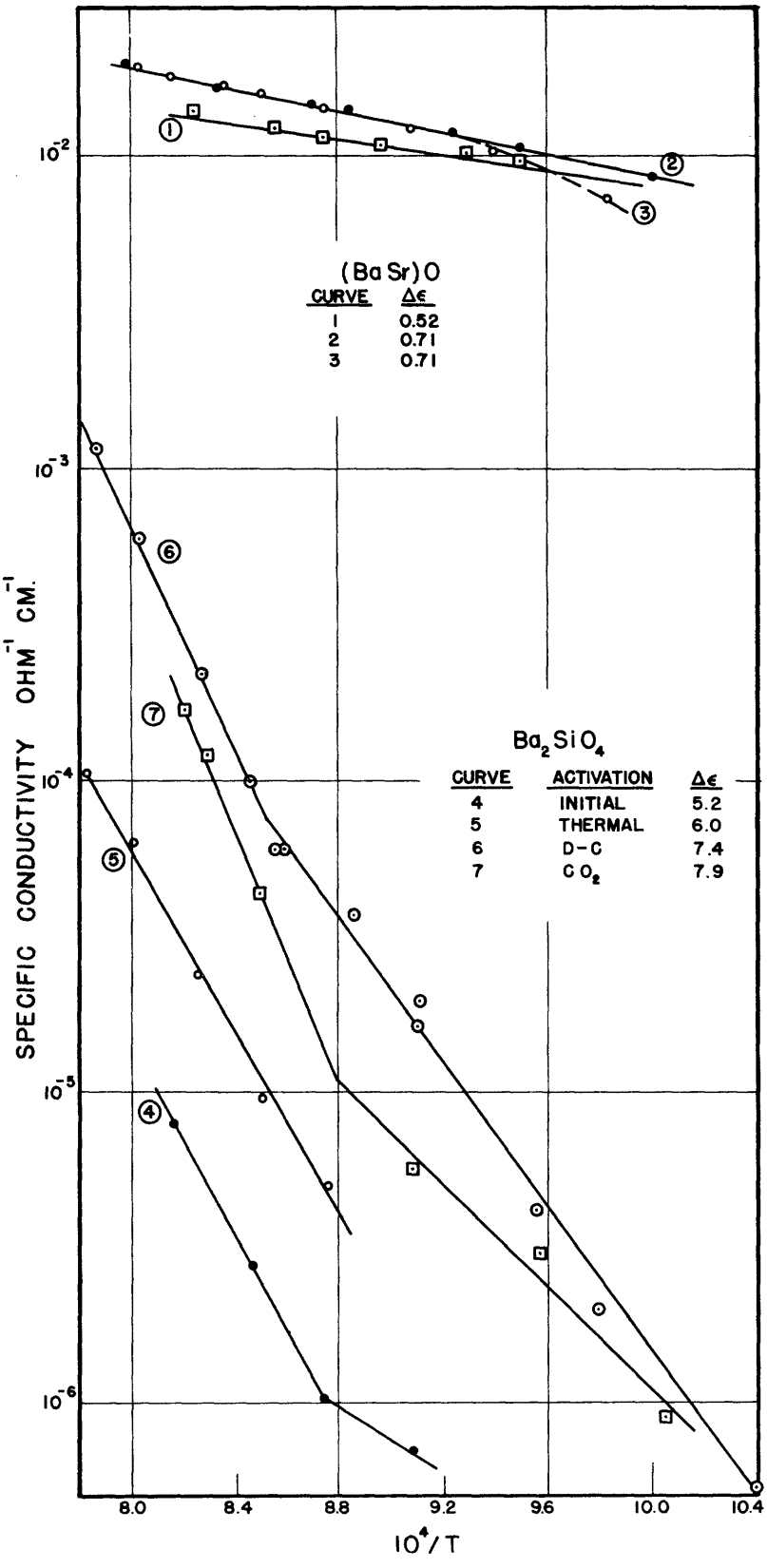

Fig. 11. Comparison of the temperature variation of the electrical conductivities of (BaSr)O and Ba_2SiO_4.

drop across this layer should manifest itself particularly at lower temperatures. The slight "break" in the conductivity curves suggests the possibility of two sources of electrons and two activation energies. Only the higher energy slopes are indicated by the $\Delta\epsilon$ values shown on the figure.

The presence of a low conductivity, high activation energy, interface layer must be considered in an energy-level representation of the complete cathode. One model which can be assumed is shown in Fig. 12. At (a), a cross-section view of the cathode places a relatively thick interface layer between the base metal and the oxide coating; (b) and (c) show energy levels present in this structure for the condition of zero current flow and for an appreciable current flow, respectively. Both the interface

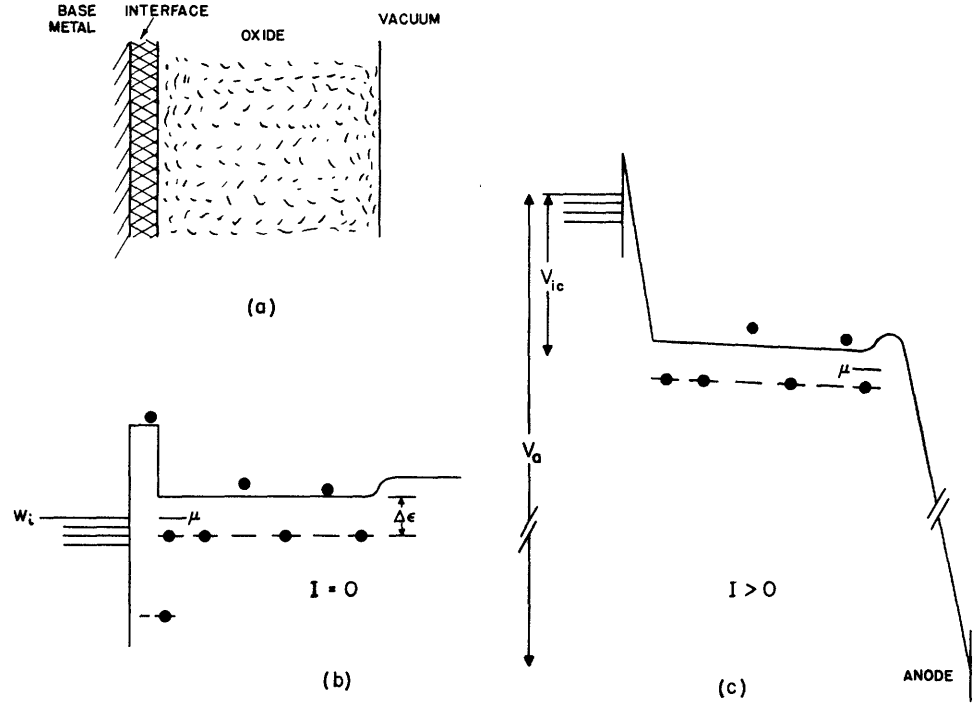

Fig. 12. (a) Cross-section view of interface type cathode, (b) energy-level representation of complete cathode for zero emission and (c) for an appreciable emission current.

and coating are assumed to be N-type, impurity semi-conductors, the activation energy of the interface being considerably larger than that of the coating. In this model the chemical potentials of the interface and coating, μ, are equated to the Fermi level in the metal, W_i. This gives rise to an energy barrier for electron passage from the base metal into the conduction band of the interface. The height of this barrier is approximately $\Delta\epsilon'/2$ with $\Delta\epsilon'$ the thermal activation energy of the interface material. Values obtained from the slopes in Fig. 11 indicate a barrier height of at least 2.5 ev. In view of the copious electron emission current densities obtainable from oxide cathodes at normal operating temperatures, this value for the barrier height may be somewhat high. The presence of excess barium

or strontium activator atoms in the complete oxide cathode may result in a somewhat lower activation energy for the barium orthosilicate present at the interface. Wright[7] has indicated a barrier height of 0.7 ev for a cathode whose base metal contained magnesium. Application of an anode voltage V_a, Fig. 12c, permits a flow of electrons through the cathode which gives rise to a tipping of the conduction bands of the interface and coating. The degree of tipping is determined by the respective electrical conductivities. The chemical potential of the oxide coating near the vacuum surface is thereby depressed below the Fermi level of the base metal by an amount V_{ic}, the potential drop through the interface and coating. Under normal d-c emission conditions this coating and interface voltage is small but under conditions of high current density, pulsed emission or low temperature, d-c operation this voltage is not negligible with respect to the applied voltage V_a.

4. Retarding-Potential Measurements

An unambigous determination of the oxide coating and interface conductivity may be made only by using the double-probe technique. This method[8,28,29] involves a measurement of the potentials developed in the cathode by two probes imbedded at different depths in the oxide coating. From a knowledge of the position of the probes within the cathode and the potentials assumed by each when an emission current is allowed to flow, the coating and interface conductivities are computed. Several serious limitations are imposed on this method. The construction of probe cathodes with accurately known probe positions is quite difficult. Cathodes raised to the sparking point frequently suffer a "burn-out" of the probe lead. Microsecond pulsed measurements cannot be extended to temperatures below about 1050°K because of the effect of time constants in the viewing circuit. Inherent capacity in the synchroscope combined with the rapidly increasing cathode resistance with decreasing temperature gives an RC time constant considerably in excess of one microsecond.

A retarding-potential method has been devised to measure the total interface and coating potential drop. Although this method does not yield directly values of the respective conductivities, these may be estimated from previous results obtained with other techniques. For temperatures below 1100°C, Mutter's [28] double-probe data indicate that the coating conductivity is probably negligible compared with the interface (barium orthosilicate) conductivity. This is confirmed in a comparison of the coating and interface specific conductivities, Fig. 11. The retarding potential method is not limited in its application and may be used at low temperatures as well as in the sparking region.

Electrons emitted with thermal energies from the surface of the cathode in Fig. 12c will arrive at the anode with an energy corresponding to

$(V_a - V_{ic})$. These electrons are allowed to pass through a small hole in the anode and their energy is measured by observing the retarding potential which must be applied to a collector placed behind the anode to just stop the electrons. The difference between this measured voltage and the applied anode-cathode voltage is then V_{ic}.

Retarding potential tubes of the type shown in Fig. 13a were used. Flat, indirectly heated cathodes+ having an area of 0.5 cm^2 were vacuum-fired at 1225°K before application of the oxide coating. A 5 per cent Si-Ni base metal was used and after vacuum-firing was coated with $(BaSr)CO_3$, (C51-2), to a weight of 10 mg/cm^2. The cathode, mounted with the emitting surface facing downward, was supported from the press of the tube on insulating glass beads. The heater and cathode leads, 1 and 2, emerged from a two-lead press at the base. A .002-in. molybdenum-nickel thermocouple, attached to the base metal, was taken from the tube on leads 7 and 8. In operation this press acted as the cold junction of the thermocouple and was immersed in a water bath. The anode and collector were each supported on glass beads from the central press and connecting leads taken from the tube on presses 3 and 6, respectively. Tantalum was used in the anode and collector construction. The anode consisted of two discs having a 2-mm separation, mounted at the upper end of a shielding cylinder. A 1-mm diameter hole allowed the passage of electrons through a nearly field-free space into the collector cylinder mounted axially inside the anode shield. A 1.5-mm diameter hole in the collector was carefully aligned with the anode hole to prevent secondary electrons arising from the bombardment of the upper surface of the collector.

The pulse circuit used in making retarding potential measurements on these tubes may be seen in Fig. 13b. A negative, one-microsecond++ pulse was applied across resistor R_2 on which taps allowed a definite fraction of the pulse voltage to be viewed and measured on a Model 4 Synchroscope. The flow of a current pulse to the anode (3) gave rise to a potential drop across the viewing resistor R_1. This voltage was likewise measured on the synchroscope. Negative d-c retarding potentials V_c were applied to the collector (6) through a galvanometer of sensitivity 10^{-10} amp/mm. Condensers C_1 and C_2, each 0.1 mfd, provided an integrating circuit allowing the average pulsed, collector current to be read on the galvanometer. Support leads 4 and 5 were connected in the circuit as shown to minimize leakage across the glass support leads. Resistor R_1 was shorted out when retarding-potential measurements were taken.

+ Cathode parts of the type used in the 2C39 lighthouse tube were kindly supplied by H. D. Doolittle, Machlett Laboratories Incorporated.

++ Link Model 9 Pulser.

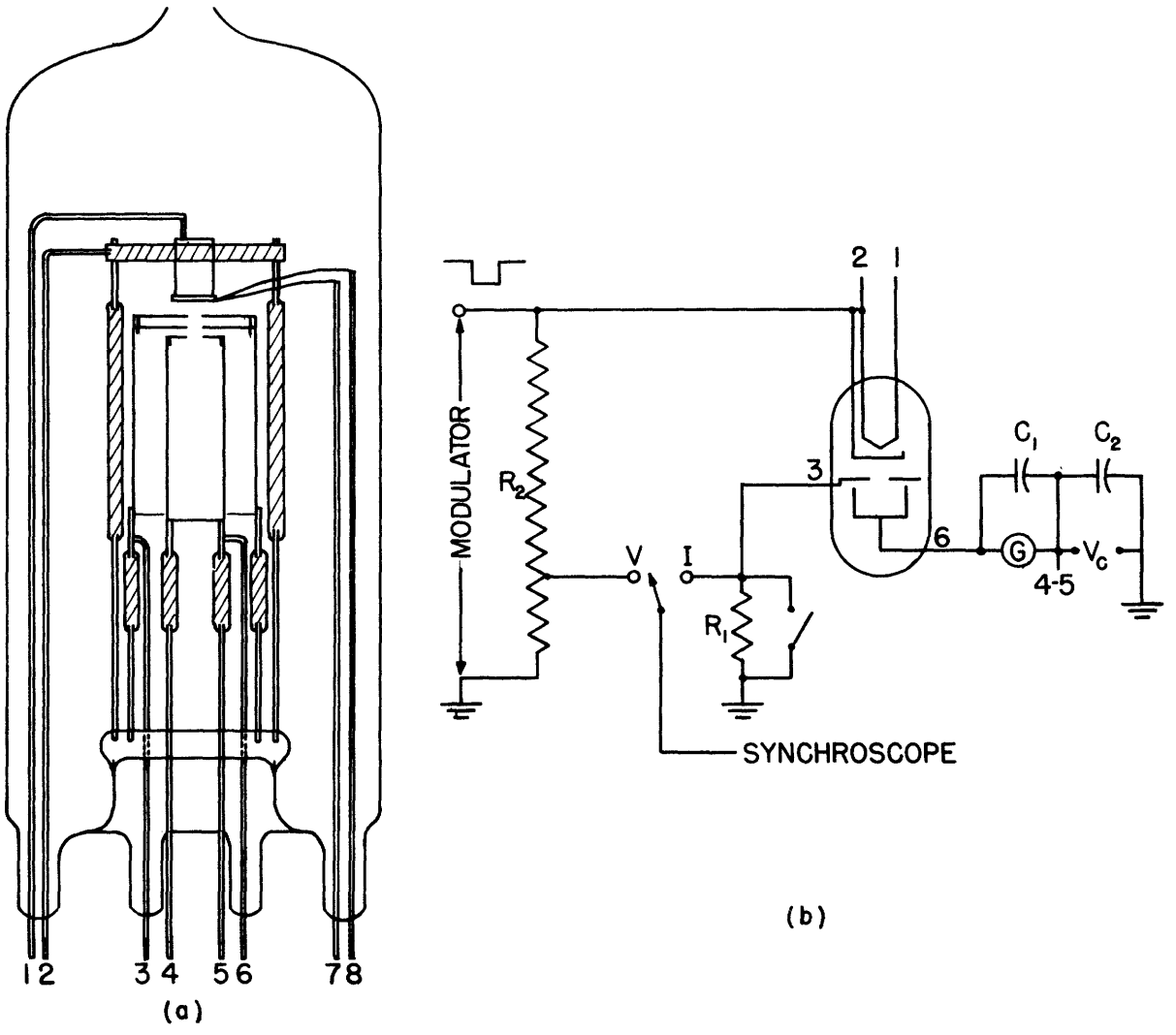

Fig. 13. (a) Cross-section view of retarding-potential tube, (b) pulsed circuit used in making retarding-potential measurements.

The procedure for evaluating the coating and interface drop V_{ic} is as follows. The cathode temperature and applied anode voltage V_a were adjusted to provide operation at a given point on the voltage-current characteristic plot. As the d-c collector potential was made negative with respect to the anode, the collector current was measured. This variation of collector current with voltage comprised the retarding potential curve and is shown in Fig. 14. The shape of this curve is closely related to the shape of the voltage pulse applied to the tube. Two pulse shapes were used and are sketched in the lower right: A is the normal 1-μsec negative voltage pulse and B is a modified pulse, formed by placing a small condenser across the output of the pulse modulator. As the potential of the collector becomes equal to, or more negative than, the potential of the emitting oxide surface, the collector current decreases rapidly. A plot of the logarithm of the collector current vs. collector voltage does not yield a linear curve of slope e/kT as it should in a simple diode retarding-potential

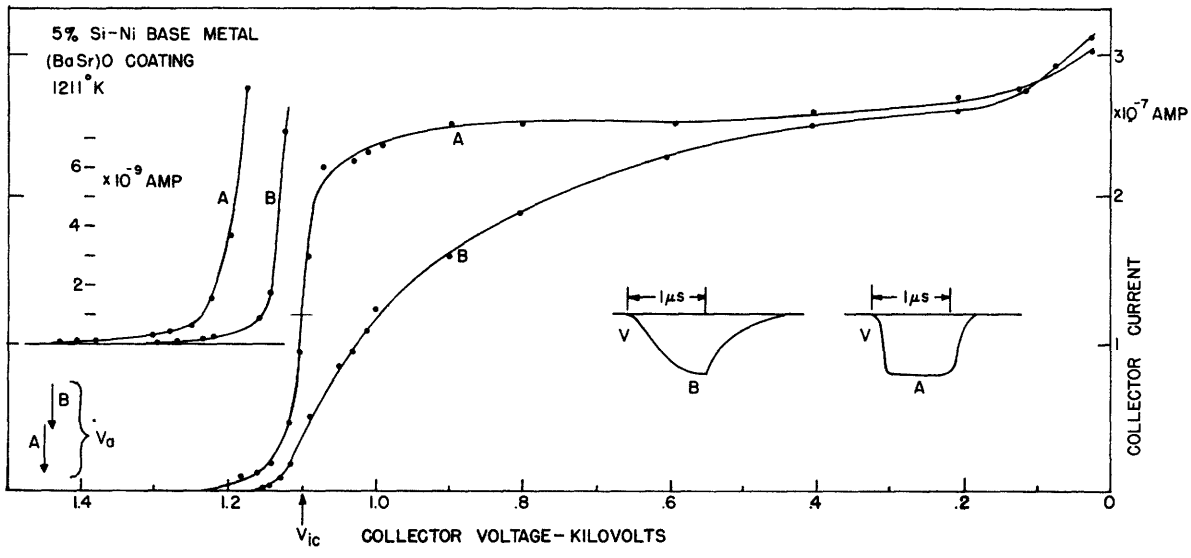

Fig. 14. Retarding-potential characteristics obtained with two differently shaped pulses.

measurement. This is due to a variation in energy of the electrons arriving at the collector resulting from the changing anode voltage during the pulse. A comparison of the retarding potential curves A and B shows this effect. When the maximum applied anode voltage V_a was 1.45 kv, see Fig. 14, voltage fluctuations on the top of pulse A amounted to about $\pm$ 15 volts. This value is sufficient to explain the rate of current decrease with retarding voltage in Curve A. The collector current does not drop sharply to zero, but has a "tail" of high-energy electrons extending out to V_a. An expanded current scale plot at the upper left of Fig. 14 shows this tail. In many cases the tail extends out to the full applied anode-cathode voltage but never beyond.

Because of the dependence on pulse shape and the presence of the tail of high-energy electrons, the usual treatment of a retarding-potential curve cannot be used. The potential of the cathode surface with respect to the anode is defined as the voltage coordinate of that point on the curve at which the collector current has decreased to half-value. This procedure defines an average measured cathode surface potential, V_m, corresponding to the average measured applied anode voltage neglecting fluctuations during the pulse, V_a. From Fig. 14, Curve A, this cathode surface potential is 1.1 kv and the coating and interface voltage

$$V_{ic} = V_a - V_m \qquad (5)$$

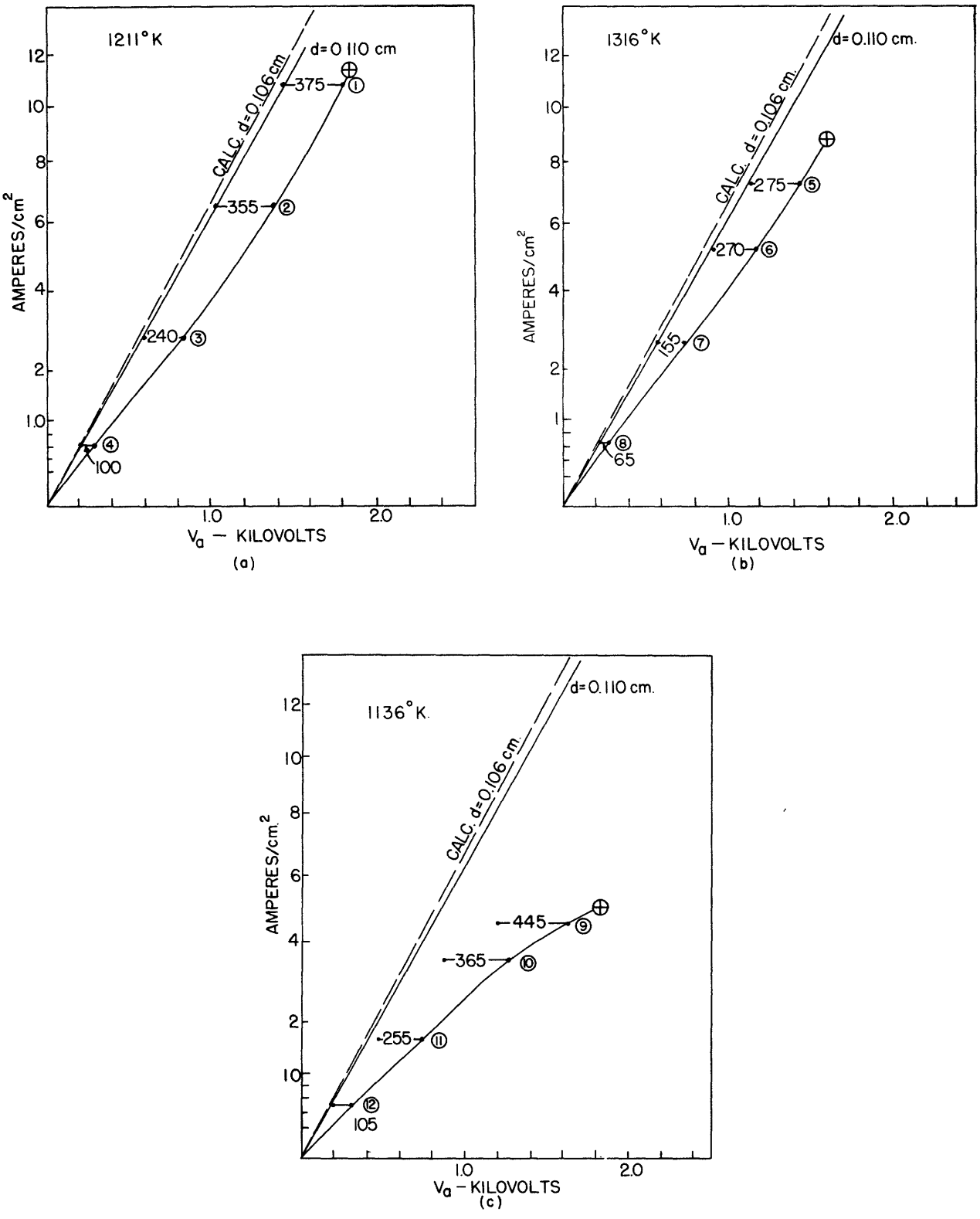

Fig. 15. Emission characteristics of retarding-potential tube at three operating temperatures.

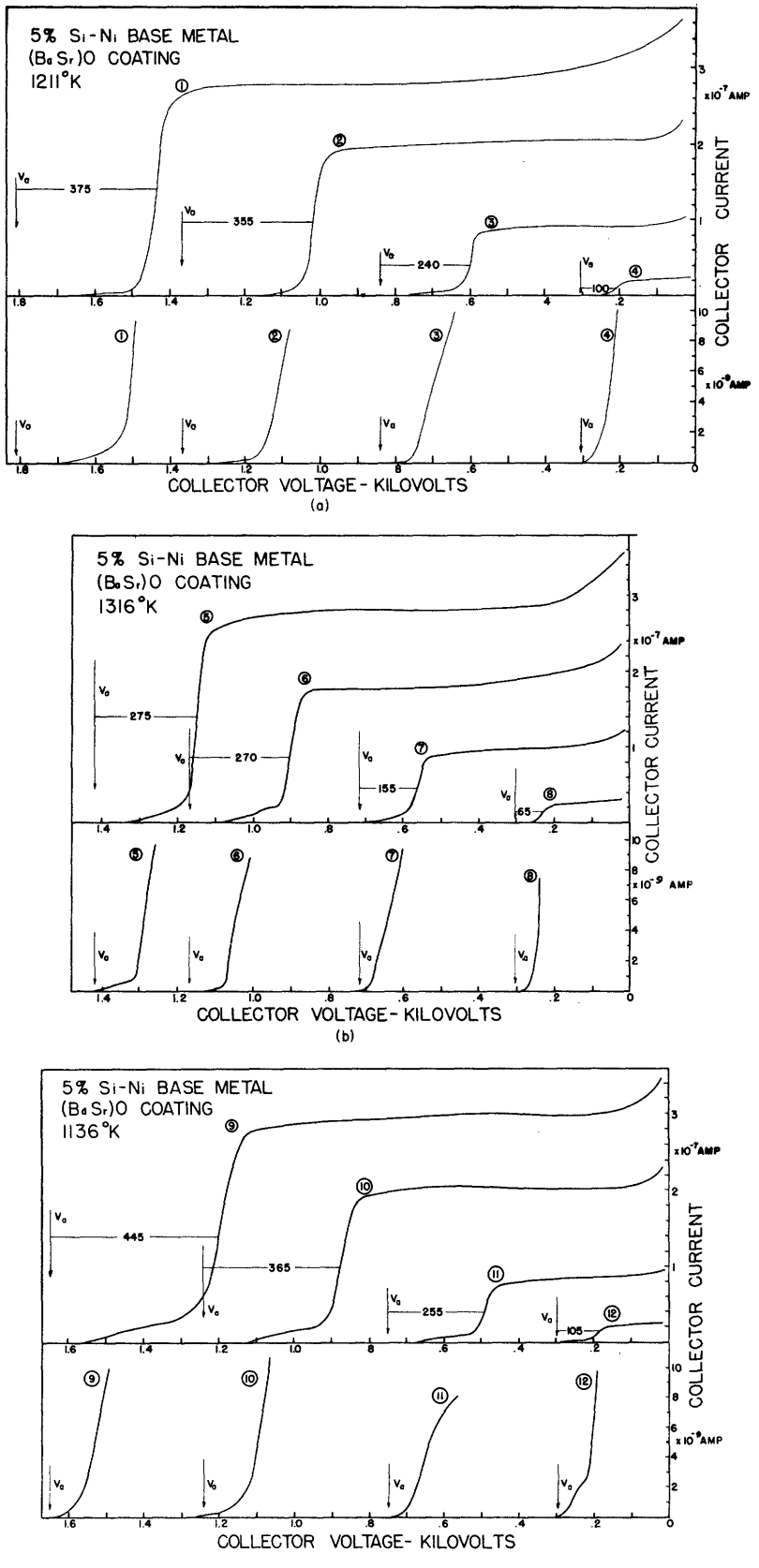

Fig. 16. Retarding-potential characteristics for three operating temperatures.

is 350 volts. Thus it is evident that the interface and coating voltage is not negligible with respect to the applied anode-cathode voltage.

The variation of V_{ic} with cathode temperature and emission current is seen in Figs. 15, 16, and is typical of data obtained on three tubes of this type. Fig. 15 a, b, c shows the variation of the anode voltage with the emission current$^{2/3}$ at three temperatures, 1211°K, 1316°K and 1136°K. Experimental points 1 through 12 define the tube characteristics and the star-marked points indicate the onset of sparking. The dashed line represents the theoretical Langmuir-Child space-charge line computed for flat anode-cathode geometry and a spacing of 0.106 cm between surfaces. This value represents the average of several measurements made at different tube orientations with the use of a magnified optical projection method. Retarding-potential curves were taken at each of the twelve operating points and are seen in Fig. 16 a, b, and c. The complete retarding-potential curves are shown in the upper section of the figures with the voltage V_{ic} indicated as the difference between V_a and V_m. In the lower section, the high-energy tails are shown on an expanded collector current scale. Values of V_{ic} obtained from Fig. 16 are applied to the corresponding experimental points of Fig. 15 as subtractive voltage corrections. In Fig. 15 a and b, this correction is just sufficient in each case to bring the points to the solid straight line which represents the theoretical Langmuir-Child space-charge line for an anode-cathode spacing of 0.110 cm. The difference between this and the measured spacing, 0.106 cm, is believed to represent an error in the spacing measurement since any non-uniformity in the geometry would result in a measurement which is too small. Thus it is found that the progressive deviation type of emission characteristic can be explained by the interface and coating voltage drop.

This voltage deviation from the theoretical space-charge line cannot always be used as a measure of V_{ic} as seen from Fig. 15c. Although the subtractive correction at point 12 allows agreement with the space-charge line, points 9, 10, and 11 do not; this indicates emission-limited conditions at the cathode surface. Unless V_{ic} is known or is negligible for a given base metal and coating combination, attempts to locate the true point of deviation from the space-charge line may seriously be hampere The use of a Schottky plot to determine the zero field emission would also be subject to error unless V_{ic} is known or is negligible.

The tail of high-energy electrons, present in all cases and extending to V_a in some, is difficult to explain without making additional assumptions. Three possible causes have been considered: (1) a time variation in the potential of the cathode surface during the pulse, (2) poor electron optics allowing electrons of the same kinetic energy to be collected or rejected depending upon their position relative to the axis of the anode hole, and (3), a real variation in the energy of the electrons

due to their emission from cracks and crevices below the normal surface of the oxide coating.

If the voltage drop in the interface and coating is due only to the resistivity of the cathode and the passage of current, the potential of the oxide surface should vary during the pulse only in accord with emission-current variations. Should this current lag the applied anode voltage because of capacitance effects in the cathode, this time effect could explain the presence of the tail. With the sudden application of the anode voltage, the cathode surface might rise to the potential V_a and then approach the potential $V_a - V_{ic}$ as the flow of current increases. Electrons emitted at the beginning of the pulse would have kinetic energy corresponding to V_a while those emitted later would have that corresponding to $V_a - V_{ic}$. To test this hypothesis, retarding-potential curves were taken with 1-μsec and 10-μsec pulses under conditions which were otherwise identical. If the tail were due to high-energy electrons emitted at the beginning of the pulse, the ratio of the tail to the total collector current should vary as the pulse length is changed. Figure 17 shows the results of this test. The 10-μsec curve is plotted on a 1/10 scale and shows reasonable agreement with the 1-μsec curve in the regions of both the tail and the total collector current. Any change in the ratio of these currents is much less than ten to one as predicted by this hypothesis.

Poor electron optics resulting in a non-uniform electric field in the region of the anode hole could cause a variation in the effect of retarding collector potentials on the electrons, depending upon their position and direction of passage through the hole. For electrons of kinetic energy corresponding to $V_a - V_{ic}$, this effect could change the shape of the retarding-potential curve near cut-off, but under no condition could it permit the arrival of $V_a - V_{ic}$ energy electrons at a collector potential approaching V_a.

Several factors seem consistent with the hypothesis of a real variation in energy of emitted electrons. A comparison of the tails of Curves A and B, Fig. 14, shows the magnitude of the tail to be associated with the duration of time that V_a remains at its maximum value, consistent with this hypothesis. A microscopic examination of oxide cathodes reveals numerous cracks and crevices in the coating resulting from a decrease in density upon conversion from the carbonate to the oxide. This is true particularly for coating weights as heavy as those used in these tubes. When the cathode is heated to operating temperature, these cracks in the coating are easily visible. Cathodes prone to frequent sparking acquire pits in the coating which in some cases extend through the coating and interface. From Fig. 14 the ratios of tail current near V_a and near the cut-off to the total collector current are about 1:1000 and 1:10, respectively. It seems reasonable to expect that 1/1000 of the coating area consists of cracks extending to the base metal and that 1/10 of the area is deeply pitted.

Although previous d-c retarding-potential measurements[30,31] are consistent with variations only in thermal energy, these measurements were made on cathodes which probably contained no interface and at currents sufficiently low that the coating voltage drop was negligible.

5. Cathode Sparking

At normal operating temperatures the electron emission from oxide cathodes is frequently limited only by the phenomena of sparking. Although a small physical loss of coating accompanies each spark, this process is generally not injurious to the cathode emission. Many cathodes appear to spark under space-charge-limited conditions[20], although a slight deviation from the true space-charge line due to a small interface and coating voltage may be undetected in these measurements. When the tube is operated in the region of sparking, measurements of V_{ic} should yield information regarding the effect of the interface on this phenomena particularly when the coating voltage is negligible.

A comparison of points 1, 5, and 9 of Fig. 15 shows that sparking does not occur at a fixed value of V_{ic} as the temperature is changed. Fig. 5b and Fig. 7 show variation of the sparking point at several temperatures and is a general characteristic of all Ba_2SiO_4 interface cathodes. If it is assumed that the voltage deviation from the space-charge line represents only V_{ic}, a correlation between sparking and the i^2R dissipation in the interface and coating is possible. The dash curve of Fig. 7a represents the products iV_{ic} = 900 watts/cm^2 and offers good agreement with the variation of the sparking points. A similar treatment of the sparking points for this cathode, Fig. 7b, shows best agreement with iV_{ic} = 4800 watts/cm^2. The three sparking points in Fig. 15 cover too small a temperature range to justify curve fitting; however, a computation of iV_{ic} yields values between 2200 and 4200 watts/cm^2.

This correlation would seem to favor a sparking mechanism based on heat energy dissipation within the cathode. Since most of the cathode resistivity is located in the interface region of thickness 10^{-3}cm, a considerable local temperature rise is expected. The above correlation (in Fig. 7) is based on the assumption that deviations from the space-charge line represent only values of V_{ic}. Points 9, 10, and 11, Fig. 15c, show that this assumption may lead to erroneous conclusions. Similarly, the agreement in Fig. 7a between the sparking point at 840°K and the dashed curve is doubtless fortuitous since this implies a 7.8 kv value for V_{ic}.

Wright[7] has assumed that the potential drop in the emitting oxide cathode occurs at the interface and has estimated the interface thickness to be such that at sparking a voltage gradient of 10^6 volts/cm exists in this region. An assumed interface thickness of 5 x 10^{-4}cm and the observed

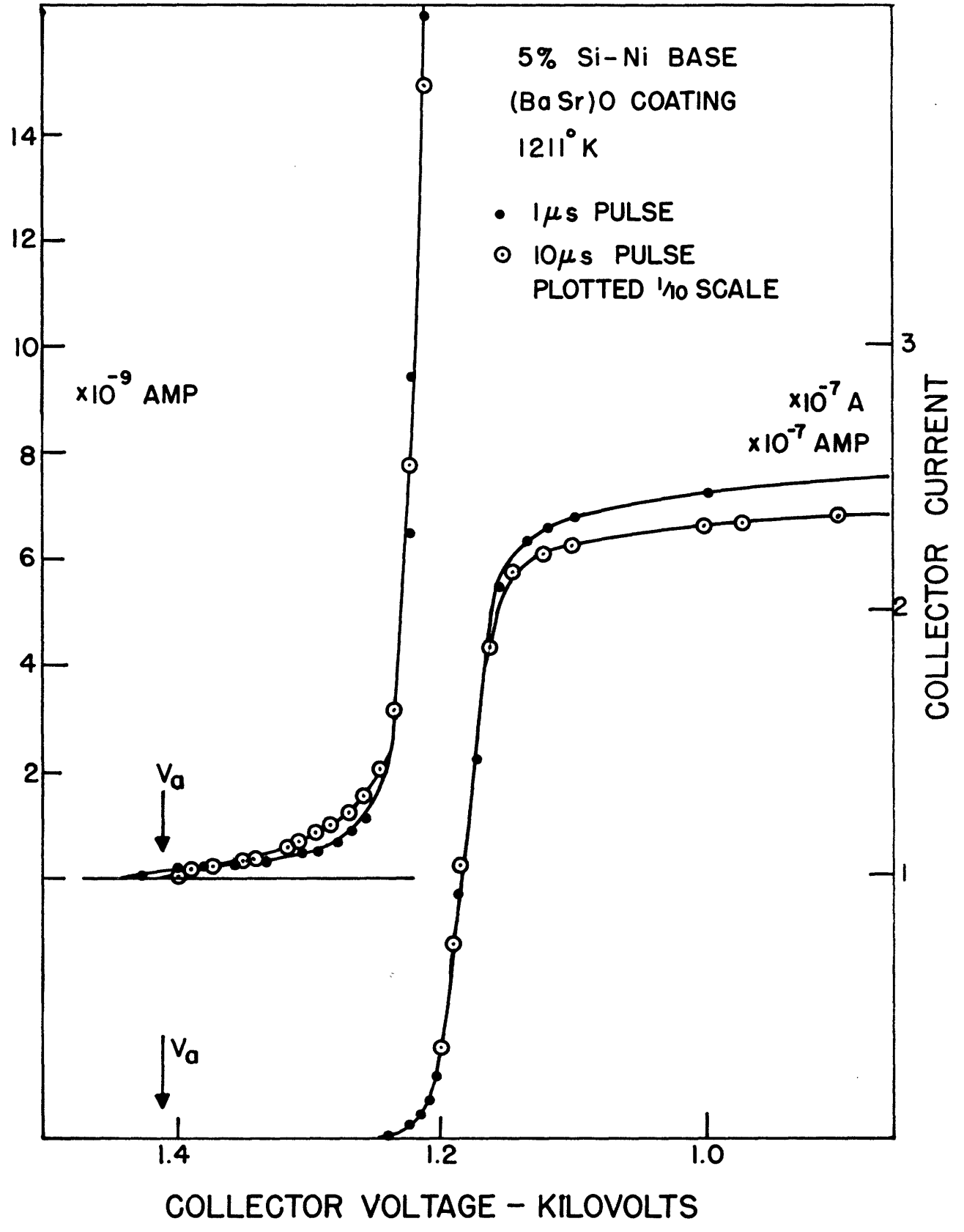

Fig. 17. Retarding-potential characteristics of 1-μsec and 10-μsec pulses.

value of V_{ic} permit a check on this estimate. Point 9, Fig. 15c, near sparking, would lead to a value of 6×10^5 volts/cm. In other measurements, values of V_{ic} up to 850 volts have been observed, leading to gradients of 1.2×10^6 volts/cm. In view of the probable existence of thin spots in the interface layer through which the voltage gradient is in excess of these average values, the fundamental mechanism of sparking may be a simple dielectric breakdown[29]. Sufficient information is not available at the present to decide between these two possible mechanisms. The presence of a definite interface compound of low conductivity is certainly responsible for sparking and accounts for the difference in sparking currents observed in Fig. 5a, b.

Acknowledgment

The author expresses his appreciation to the Frank B. Jewett Fellowship Committee and to the Research Laboratory of Electronics whose joint support made this work possible.

References

1. N. F. Mott and R. W. Gurney, "Electronic Processes in Ionic Crystals," Oxford University Press, (1940), p. 176.
2. J. R. Dillinger, University of Wisconsin, Ph. D. Thesis (1947).
3. A. Eisenstein, Phys. Rev. 71, 473 (1947).
4. H. P. Rooksby, J. Roy. Soc. Arts, 88, 318 (1940).
5. H. P. Rooksby, J. Gen. Elec. Co. 11, 83 (1940).
6. H. P. Rooksby, Nature 159, 609 (1947).
7. D. A. Wright, Proc. Roy. Soc. Lond. 190, 394 (1947).
8. A. Fineman, and A. Eisenstein, J. App. Phys. 17, 663 (1946).
9. H. O'Daniel and L. Tscheischwili, Z. Kristallogr. 104, 348 (1942).
10. D. A. Wright, private communication.
11. A. Eisenstein, J. App. Phys. 17, 874 (1946).
12. G. Grube and R. Trucksess, Z. Anorg. Chem. 203, 84 (1932).
13. P. Eskola, Amer. J. Sci. (5) 4, 331 (1922).
14. M. Benjamin, Phil Mag. 20, 1 (1935).
15. E. M. Wise, Proc. I. R. E. 25, 714 (1937)
16. E. F. Lowry, Phys. Rev. 35, 1367 (1930).
17. A. Eisenstein, Paper in "Advances in Electronics", Academic Press, N. Y. (1948) (in press).
18. H. Jacobs, J. App. Phys. 17, 596 (1946).
19. H. C. Hamaker, H. Gruining, and A. H. Aten, Philips Res. Rep. 2, 171 (1947).
20. E. A. Coomes, J. App. Phys. 17, 647 (1946).
21. See A. Eisenstein, J. App. Phys. 17, 654 (1946).
22. R. L. Sproull, Phys. Rev. 67, 166 (1945).
23. See J. P. Blewett, J. App. Phys. 10, 668 (1939).
24. F. Seitz, "Modern Theory of Solids", McGraw Hill, New York (1940) p. 191.
25. C. H. Prescott and J. Morrison, J. Amer. Chem. Soc. 60, 3047 (1938).
26. B. R. A. Nijboer, Proc. Phys. Soc. Lond, 51, 575 (1939).
27. C. Herring, Phys. Rev. 73, 1238 (1948).
28. W. E. Mutter, Phys. Rev. 72, 531 (1947).
29. W. E. Danforth, Bartol Research Foundation, journal article (in publication).
30. W. Heinze, and W. Hass, Z. Techn. Phys. 19, 166 (1938).
31. H. Y. Fan, J. App. Phys. 14, 552 (1943).